NTNU
Norwegian University of
Science and Technology

Wind Farm Control Methods - Yawing

John Magne Gitmark

Master of Science in Mechanical Engineering
Submission date: June 2016
Supervisor: Lars Sætran, EPT

Norwegian University of Science and Technology
Department of Energy and Process Engineering

NTNU
Norwegian University
of Science and Technology

Department of Energy
and Process Engineering

EPT-M-2016-43

MASTER THESIS

for

Student
John M Gitmark

Spring 2016

Wind farm control methods - Yawing

Kontrollmetoder for vindfarm - Yawing

Background

In standard conditions a wind farm operator will exploit its assets at maximum financial optimum. This will practically result in maximizing the power production of the wind farm. In certain cases, however, reasons arise that the operator wants or is required to limit this production to a sub-maximum level.

Control Methods

We are here interested in looking at the technical mechanisms to control the power production in a wind farm.

Pitching. Pitching of the blades leads to a decrease in power, ensuring that the generator will not get overloaded. The same aerodynamic principle can be used before rated power, in order to reduce the wind power. An increase in the pitch angle, will lead to a lower power production. While applying the pitching mechanism, the rotor speed is kept constant, so the power production will drop.

Over-speeding. The second common method of wind power control is to allow the rotor to speed to increase above its optimal point

Yawing. A third mechanism is yawing the rotor out of the wind from its optimal point. When looking at the effect of yawing on the power coefficient there is, however, much more debate than with the previous two methods. When the turbine is in yawed position, the blades of the rotor endure an extra cyclic load due to the in-plane velocity component. Another effect of yawing a wind turbine is that one actually may, by this action, be able to guide/lead the wake from an upstream turbine such that the wake does not hit a down-wind turbine. The down-wind turbine may therefore be exposed for wind that has a larger energy potential than what is in the wake from the up-wind turbine.

Here, we like to study the effects of yawing the turbine. There exist 2 model wind turbines in the Aerodynamics Laboratory, that can be used for experiments in the Large Wind Tunnel. The wind turbine models are equipped with sensors for measuring torque and rotational speed, and the wind tunnel has equipment for thrust measurement and a diversity of equipment for measuring velocity characteristics in the turbine wakes.

-- ” --

Within 14 days of receiving the written text on the master thesis, the candidate shall submit a research plan for his project to the department.

When the thesis is evaluated, emphasis is put on processing of the results, and that they are presented in tabular and/or graphic form in a clear manner, and that they are analyzed carefully.

The thesis should be formulated as a research report with summary both in English and Norwegian, conclusion, literature references, table of contents etc. During the preparation of the text, the candidate should make an effort to produce a well-structured and easily readable report. In order to ease the evaluation of the thesis, it is important that the cross-references are correct. In the making of the report, strong emphasis should be placed on both a thorough discussion of the results and an orderly presentation.

The candidate is requested to initiate and keep close contact with his/her academic supervisor(s) throughout the working period. The candidate must follow the rules and regulations of NTNU as well as passive directions given by the Department of Energy and Process Engineering.

Risk assessment of the candidate's work shall be carried out according to the department's procedures. The risk assessment must be documented and included as part of the final report. Events related to the candidate's work adversely affecting the health, safety or security, must be documented and included as part of the final report. If the documentation on risk assessment represents a large number of pages, the full version is to be submitted electronically to the supervisor and an excerpt is included in the report.

Pursuant to “Regulations concerning the supplementary provisions to the technology study program/Master of Science” at NTNU §20, the Department reserves the permission to utilize all the results and data for teaching and research purposes as well as in future publications.

The final report is to be submitted digitally in DAIM. An executive summary of the thesis including title, student’s name, supervisor's name, year, department name, and NTNU's logo and name, shall be submitted to the department as a separate pdf file. Based on an agreement with the supervisor, the final report and other material and documents may be given to the supervisor in digital format.

X☐ Work to be done in lab (Water power lab, Fluids engineering lab, Thermal engineering lab)
☐ Field work

Department of Energy and Process Engineering, 13. January 2016

Olav Bolland
Department Head

Lars Sætran
Academic Supervisor

Investigation of the rotational effects on the wake behind a wind turbine in yaw

John Magne Gitmark, *Norwegian University of Science and Technology, 2016.*

***Abstract*—The wake effect of yawing an upstream turbines is of interest in order to increase power production. In this study, the case of yawing is considered as asymmetric do to the tower and rotor rotation, and measurements have been performed in a wind tunnel. The rotational effects when yawing are obtained by investigating the difference between a disc and a rotor with the same drag and diameter. This is performed during a tower-symmetrical setup, and shows that the wake deflects approximately 1 radius for the disc and significantly less for the rotor at optimal tip speed ratio. The disc wake is similar to a jet shape in a crossflow and counter-rotating vortices are present, which is not the case for the rotor.**

Moreover, the differences between yawing in the different direction are investigated and show that for positive yaw-angles, the wake spreads more out and deflects more to the side and to the floor. Furthermore, for negative yaw-angles, the wake is located closer to downstream the rotor centre. These differences are slightly less present during shear flow conditions, in addition to a more sideways deflected wake.

***Keywords*—Yaw, wind turbine, wake, wind tunnel, rotation, disc.**

I. Introduction

It is a well known fact that wakes behind wind turbines may lead to wind velocity deficit and power reduction for downstream turbines, and therefore important to understand the related physics in order to design and control wind farms. Much research has been performed regarding wakes in wind farms, and [1] is an example. Additionally, [2] found that due to the atmospheric boundary layer, the economy based optimal spacing is 15 rotor diameters (D), despite the commonly used spacing of 7D. Natural wind conditions usually involve turbulence, and is desired to investigate due to more mixing. Therefore, a relation between turbulence and the output effect is revealed in research performed by [3].

As a solution to the physical challenges regarding the wake velocities, there are different ways to control the power production of individual turbines to gain a higher overall power production. One example is [4] who investigated the effect of yawing the downstream turbines. It is also possible to influence the overall efficiency by reducing the power production of the upstream turbines, and [5] did wind tunnel experiments by changing the tip speed ratio and blade pitch of an upstream turbine, resulting in increased overall power output.

In addition, it is possible to yaw the upstream turbine, which has been done by [6], [7], [8], [9] and [10]. In the experiment of [6] it was found that the wake deflects to the side, depended of the yaw-angle and downstream distance. Moreover, [7] investigated the performance of a turbine placed 3D downstream of a yawed turbine. They found that under these conditions, the optimal yaw-angle of the first turbine is approximately 30°. Both [8] and [10] did wind tunnel experiments with a shear flow, which is important since the flow is similar to real conditions. [8] compared results for laminar and turbulent inflows and found that for a spacing distance of 2D, the optimal yaw-angle for laminar flows is 10°. However, with a turbulent flow, yawing did not yield any positive results. [10] used PIV to track the wake up to 12D and found that the wake recovery is asymmetrical. A near wake study was performed by [9] who also investigated the outcome for high and low tip speed ratio under yawed conditions.

The yaw misalignment may also affect the outcome when not wanted. [11] assume a RMS of 10° for yaw misalignment during a time period of 10 minutes, based on measurements. This is another reason why it is needed to better understand the effect of yawing.

CFD simulations are frequently used to predict wakes, and [12]'s simulation resulted in a difference between positive and negative direction of yaw rotation. The results from this has also been used in [13] for power optimization by yaw controlling, and a yaw-angle of approximately +20°(direction to be defined) is presented as optimal for 7D spacing. A few years earlier, [14] did a LES simulation of wakes during yaw. According to them, discs are occasionally used to simulate turbines, hence, a disc is used in their simulation.

Discs have also been used to simulate rotors in wind tunnel experiments, as is excellently shown in [15]. In this paper, the wake of a small scale porous disc in yaw was investigated at hub hight and in stream wise cross sections. The 2-dimensional contour plots of the cross sections show a curled wake resulting from counter-rotating vortices. These vortices are shown experimentally by the span wise velocity. Furthermore, both the stream wise and span wise velocity component are highly depended on the height of the measurements. The counter-rotating vortices are also revealed in a following LES simulation of the disc showing the vertical velocity component as well. The measured wake centre at hub height matches the LES simulations of a disc in [14]. Additionally, a LES simulation of a rotating turbine is performed and the results show a small mismatch to the disc, however, the wake is still curved and deflected. This last simulation did not include a tower.

In this study, the difference between a drag disc and a rotating turbine will be investigated in wind tunnel experiments. Furthermore, the difference between positive and negative yaw

J. M. Gitmark is a master student at the Department of Engergy and Process Engineering, Norwegian University of Science and Technology, Trondheim, Norway, e-mail: john.m.gitmark@gmail.com

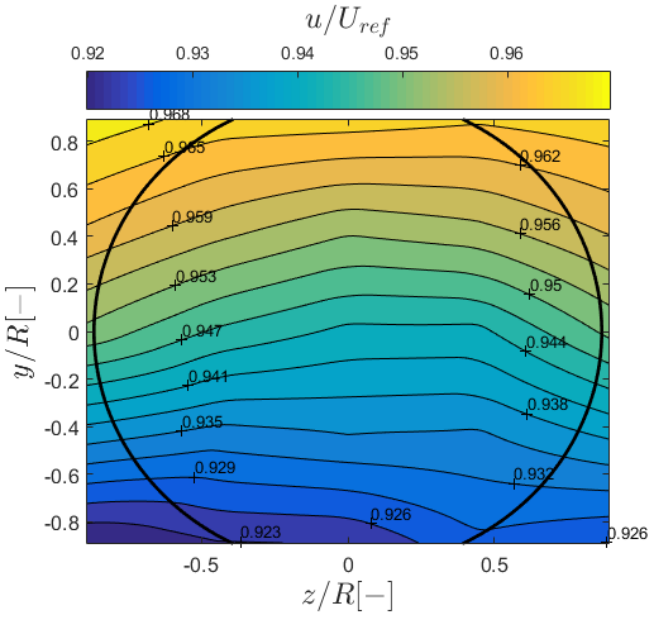

Fig. 1. The normalized profile of the shear flow. U_{ref} is a reference velocity measured at the contraction. The black circle represents the rotor in 30°yaw.

direction is taken into account, supported by [12] and [13]. It is believed that this asymmetrical behaviour is due to the turbine tower together with the direction of rotor rotation. The setup for this experiment is therefore symmetric regarding the towers, which will be explained in more detail in the next chapter. This will later be refereed to as "experiment 1".

Additionally, the wake behind a yawed rotor in an asymmetrical regular setup is investigated for both directions of yaw, under laminar, turbulent and shear flow conditions (experiment 2).

II. Methodology

A. Experimental setup

The experiments are executed in a wind tunnel at the Norwegian University of Science and Technology (NTNU). The test section is 11 meter long, 1.8 meter high and 2.7 meter wide. A contraction is placed at the inlet to produce a plugged wind profile during laminar flow condition. Turbulence and shear flow for experiment 2 are created by placing grids at the inlet with regular and irregular spacing, respectively. The turbulence intensity is between 4% and 5% for both turbulent flow and shear flow. The normalized velocity profile of the shear flow, where U_{ref} is a temporary reference velocity measured at the contraction, is plotted in Fig. 1. The average values of all y=constant are used to curve fit according to the power law, resulting in an exponential value of $\alpha = 0.0917$. The calculated velocity at the rotor centre height is used as the final reference velocity (U_{ref}). More details about the grids can be found in [16].

The rotor is 3D-printed, has diameter of 450mm and was mounted on a hub with a diameter of 82mm and a length of 550mm. The hub is resting on a tower with a varying diameter

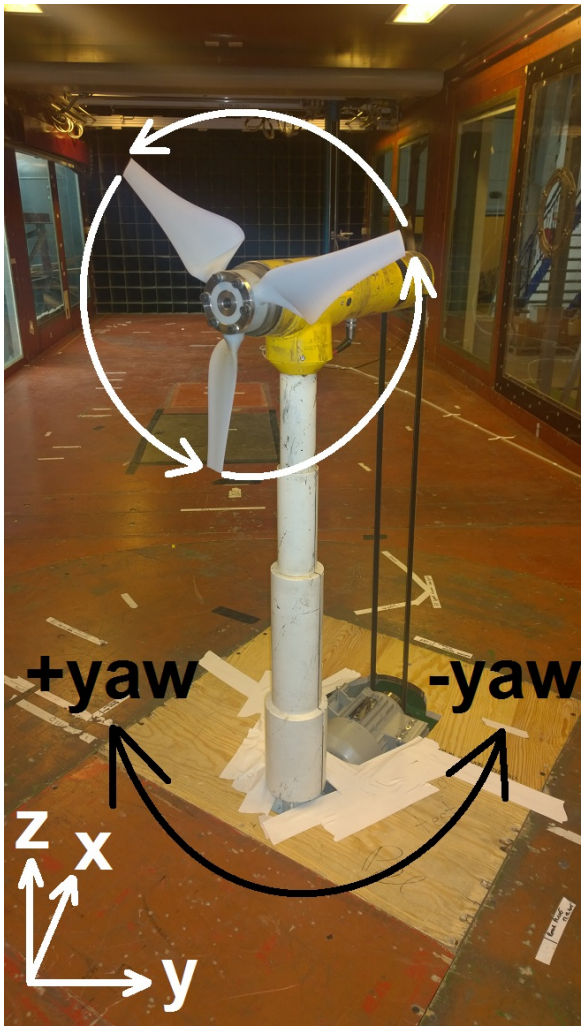

Fig. 2. The coordinate system and rotor seen from the inlet during yaw in positive direction.

of 46mm-100mm (Fig. 2). A more detailed description of the hub and tower is found in [17] (note the different rotor-size). The turbine is placed on a rotatable 6-component force balance. The centre of the rotor, which also is the origin in the coordinate system is placed above the centre of the balance. This means that the rotor always will be in the centre, independent of the yaw-angle. It should be noted that the rotor is small compared to the hub and tower. Nevertheless, there are strong advantages by using a downscaled rotor to overcome wall effects during yaw, due to lower blockage. Hence, a smaller rotor is used in the experiments.

The disc used in experiment 1 has the same drag force as the rotor at optimal tip speed ratio. It is made by two wooden discs fasten together and adjusted by tape to get the exact same drag. In order to make the symmetrical setup described in the introduction, an additional tower is placed between the hub and the roof (Fig. 3). In this way, the direction of yaw is independent of the result. To make the setup as

Fig. 3. The disc attached to the turbine with additional tower on top at 30°yaw. Note that the belt was taken off during measurements for symmetry.

symmetric as possible, the transmission belt is removed during the measurements of the disc. This is however not possible when using the rotor, which may cause smaller differences to the result. The rotor is placed in the exact same position as the disc for comparison.

In experiment 2, the positive and negative direction of yaw need to be defined. The definition of the coordinate system (x, y and z), rotor rotation direction and yaw-angle (γ) is shown in Fig 2 in front view and in Fig 4 form above.

All wakes in this experiment are measured horizontally along the z-axis at hub height 3D, 6D and 9D downstream. Due to findings in initial studies, the yaw-angle of $\pm 30°$is chosen as the main focus. Wake profiles for turbulent and shear flow conditions are also obtained for these angles of yaw. Nevertheless, during laminar flow condition, wake profiles for $\pm 10°$, $\pm 20°$and $\pm 40°$ of yaw is also measured at the same distances. More important, to fully understand the behaviour of the wake for both positive and negative yaw-directions, 2-dimensional contour plots are made for the complete cross section at 6D during laminar flow conditions.

B. Data acquisition

The wind velocity for the wind tunnel is measured by using pressure taps at two different cross sections in the inlet contraction. The pressure difference is measured by a pressure

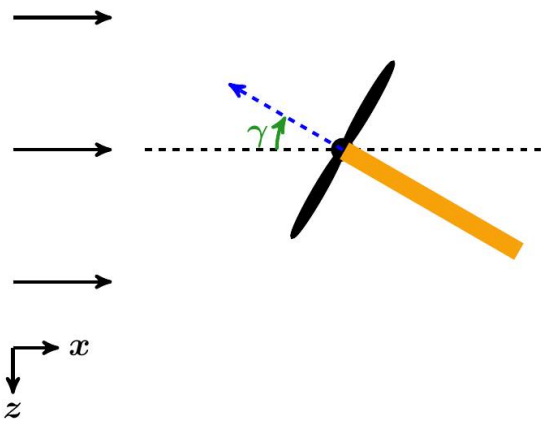

Fig. 4. The coordinate system and rotor seen from above during yaw in positive direction.

transducer and converted to an electrical signal, then amplified and filtered before converted to a digital signal in a 16 bit DAQ. The digital signal is logged into a computer by using Labview. The pressure transducer is calibrated by using an inclined manometer.

A two component laser Doppler velocimetry (LDV) from Dantec Dynamics is mainly used to collect data for the wake velocity. Series of 50,000 samples obtained during a time period of generally 20-30 seconds has been taken, and free stream velocity was logged simultaneously.

Nevertheless, a constant temperature Hot wire system from Dantec Dyamics has also been used for some of the measurements. The Hot wire system was calibrated with a pitot probe and temperature corrected according to [18]. The output signal was unfiltered and not amplified before converted to a digital signal.

The Hot wire measurements and the LDV measurements have been compared for validation, with matching results. Both were separately mounted to a travers when used.

C. Uncertainties

There are some uncertainties in the experiment, and the main sources are the calibration of the pressure transducers and the hot wire system. Except for the LDV, the same equipment are used in [19] and for wake measurements behind a turbine, the uncertainty for the normalized velocity (u/U_{ref}) is approximately 4% with a 95% confidence interval. Furthermore, the uncertainty value for LDV measurements is expected to be less due to high sensitivity and no need for calibration.

III. Results

A. Power output

C_P-values and C_T-values for yaw-angles between -50° and +50° have been measured. The C_P-curve and C_T-curve for $\gamma = 0°$ are plotted in Fig. 5 and Fig. 6, respectively. The optimal tip speed ratio of approximately 3.4 is revealed, which is the chosen rotational speed during the study. Moreover,

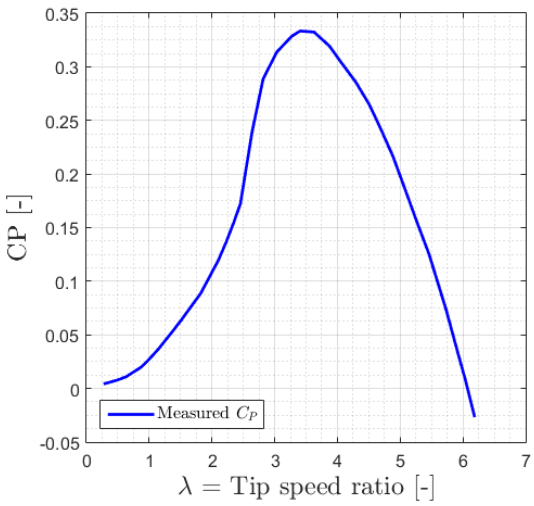

Fig. 5. The C_P-curve for $\gamma = 0°$.

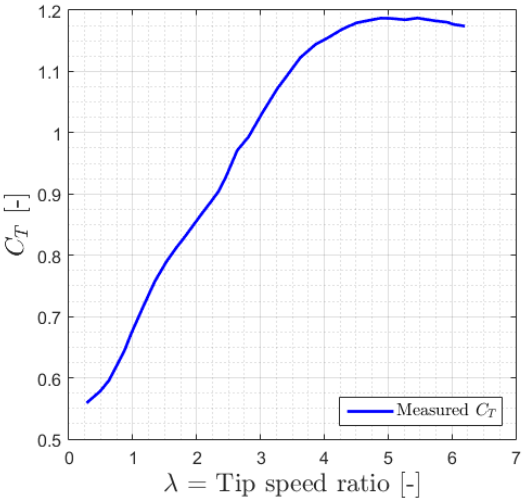

Fig. 6. The C_T-curve for $\gamma = 0°$.

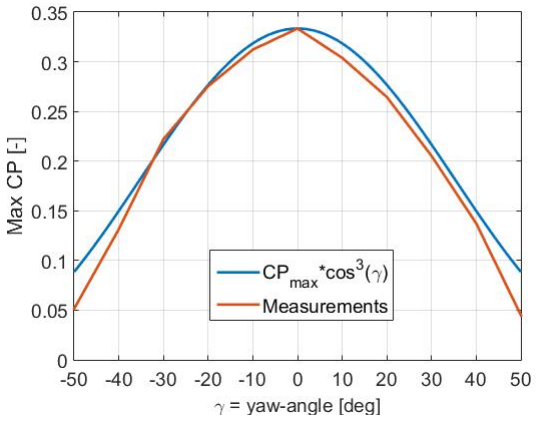

Fig. 7. The maximum C_P for different yaw-angles.

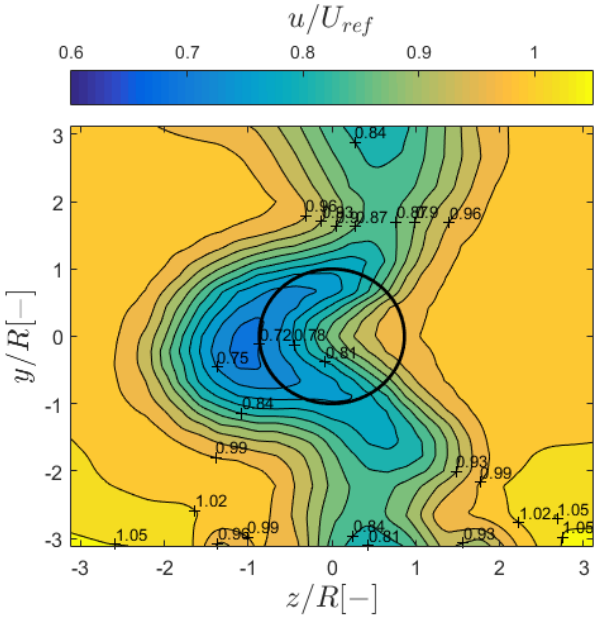

Fig. 8. The mean stream wise velocity of the drag disc, $\gamma = 30°$, x=6D.

the maximum value of C_P for all values of γ are plotted together in Fig. 7. As can be seen, the power output is close to $C_{P,max}(\gamma = 0) \cdot cos^3(\gamma)$, as expected [10]. Note that the power is slightly lower for positive yaw-angles compared to negative yaw-angles, which also is the case in [12].

B. Experiment 1

The focus in experiment 1 is to investigate the effects caused by rotation, and is performed by measuring the wakes behind a disc and a rotor. A two dimensional wake profile of the stream wise mean-velocity and span wise mean-velocity of the disc at 6D is plotted in Fig. 8 and Fig. 9, respectively. The black circle in the centre represents the yawed disc. Each plot consists of 545 measuring points with a spacing of 50mm in the wake region.

In the stream wise velocity plot (Fig. 8), the tower wakes are visual between $z/R = 0$ and $z/R = 1$ at both the top region and the lower region. Furthermore, when analysing the curled wake of the disc, it can be seen that the wake centre (maximum deficit) is shifted approximately one radius to the left at hub height. Moreover, the wake is symmetric about the z-axis. To validate, this measurement taken at 6D is between the boundaries of the results [15] obtained at 5D and 8D. The results in [15] are however not as symmetrical as in this study, which is believed to be caused by the tower-asymmetry.

The span wise velocity downstream of the disc centre shows a velocity component pointing towards the direction of wake deflection(in Fig. 9), and velocity components pointing in the opposite direction above and below. Again, this is confirmed by findings in [15], and counter-rotating vortices are expected to

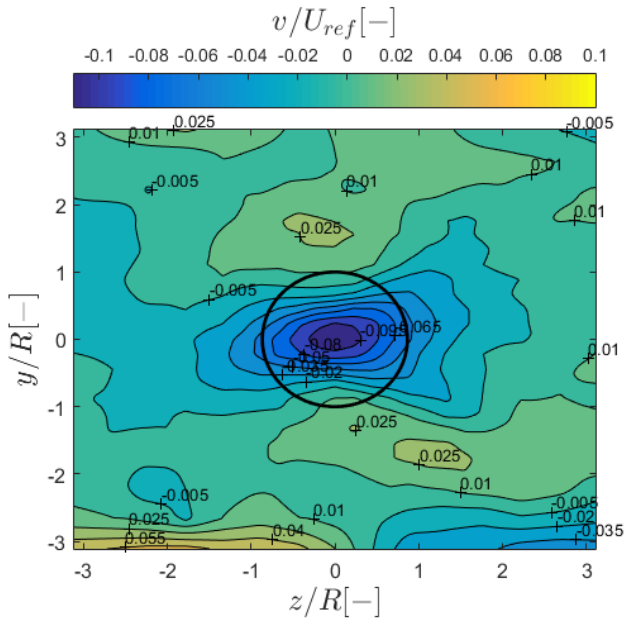

Fig. 9. The span wise velocity of the drag disc, $\gamma = 30°$, x=6D.

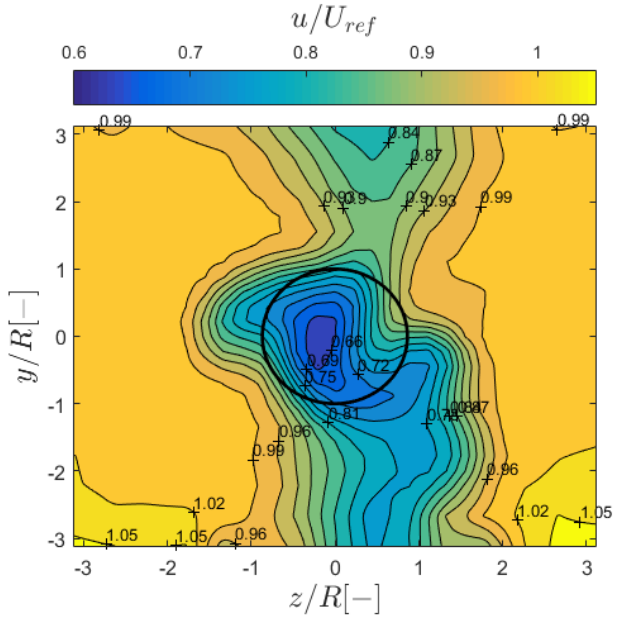

Fig. 10. The mean stream wise velocity of rotor in symmetric setup with two towers, $\gamma = 30°$, x=6D.

be present, resulting in the curled shape of the wake. The wind also tend to move towards the vertical centre for $y/R = -2.5$ to -3, as expected for a flow around a cylindrical tower.

The wake shape is also the same as the expected shape of a jet in a crossflow [20]. Similar, the flow shape is a product of counter-rotating vortices, and is according to [21] caused by a pressure difference at the leeward side. To find if this holds for the disc as well, the pressure at the downstream side of

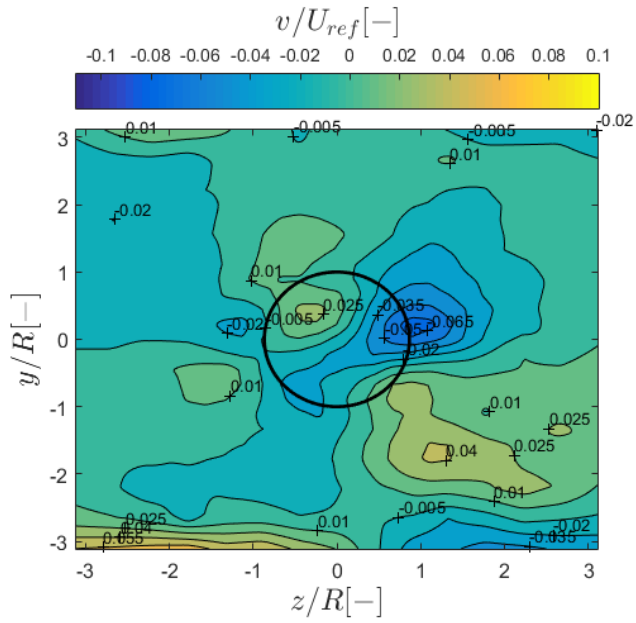

Fig. 11. The span wise velocity of rotor in symmetric setup with two towers, $\gamma = 30°$, x=6D.

the disc needs to be measured, which is not performed in this study.

The same plots have been made after replacing the disc with the rotor, and the stream wise velocity and the span wise velocity can be found in Fig. 10 and Fig. 11, respectively.

One of the most significant differences between the disc and the rotor wake is the position of the wake centre. For the rotor, the wake is positioned close to the centre, and has therefore moved almost one radius compared to the disc-measurements. The lower tower wake is also stronger than the top tower wake, and since the attached belt is the main geometrical difference between the towers, it is a possible reason. The rotor wake also tends to more towards the lower tower, and it is unclear if it is only due to the stronger tower wake, or if the rotor rotation also plays a part.

The magnitude of the span wise velocity in Fig. 11 is much lower than the velocities for the disc. Neither is there a clear pattern of positive and negative velocities, believed to cause the highly reduced wake deflection in Fig. 10.

The measured rotor wake is different from the CFD-simulated result in [15] of a rotor without any towers. This shows that the combination of a rotating rotor and blockage due to towers may reduce the wake deficit significantly. Nevertheless, the over dimensioned tower and hub should be kept in mind, believed to enhance the effect. A smaller hub and tower is recommended for further research to validate the CFD-simulation of the rotor in [15].

C. Experiment 2

The main focus in experiment 2 is to investigate the difference of yawing in positive and negative direction. To better understand the phenomena, measurements of the cross section

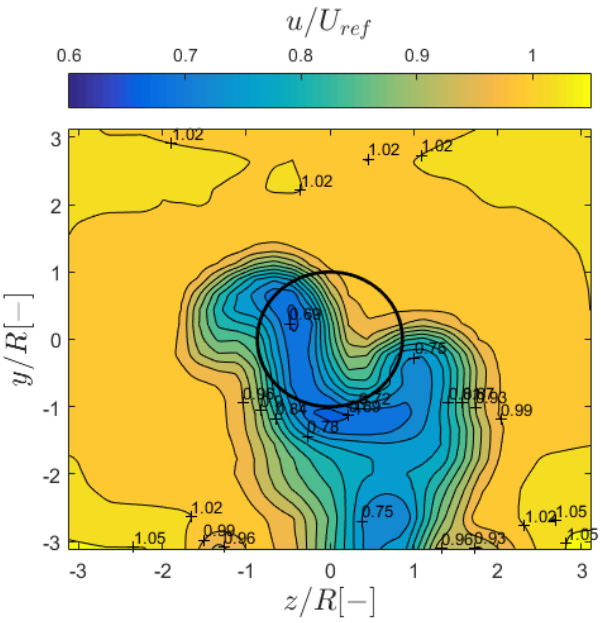

Fig. 12. The mean stream wise velocity of rotor in asymmetric setup, $\gamma = +30°$, x=6D.

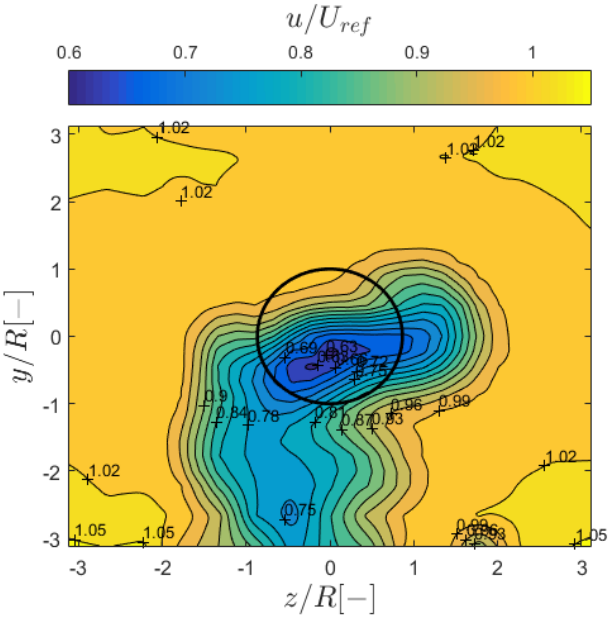

Fig. 13. The mean stream wise velocity of rotor in asymmetric setup, $\gamma = -30°$, x=6D.

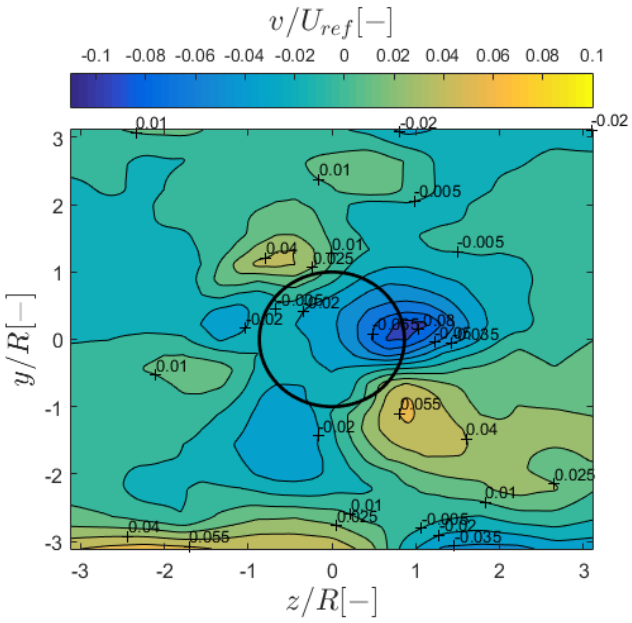

Fig. 14. The span wise velocity of rotor in asymmetric setup, $\gamma = +30°$, x=6D.

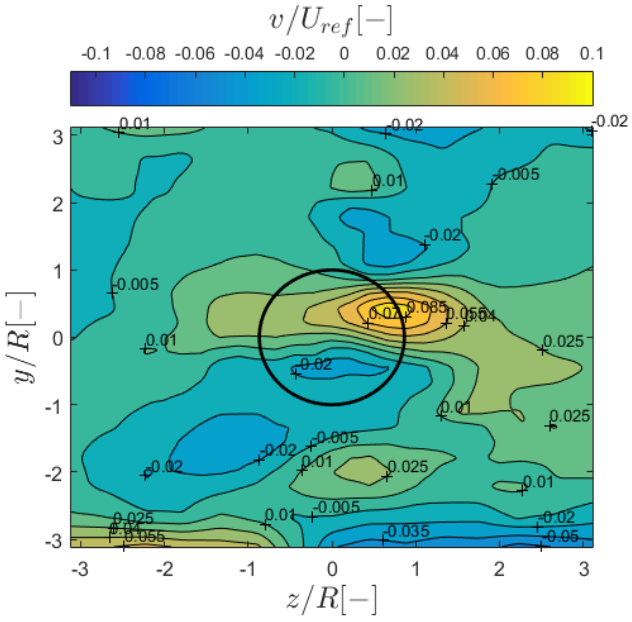

Fig. 15. The span wise velocity of rotor in asymmetric setup, $\gamma = -30°$, x=6D.

at x=6D for both $\gamma = +30°$ and $\gamma = -30°$ have been taken and stream wise velocities are plotted in Fig. 12 and Fig. 13, respectively.

The situation when yawing in the positive direction is by no doubt complicated. From Fig. 12, the wake tends to "wrap around" the centre. A large part of the rotor wake is moved downwards, while the remaining is shifted approximately 0.5R towards the side. The "hump" located about $z/R = 1$, $y/R = 0$ is most plausible caused by the hub.

The span wise velocity plot in Fig. 14 is similar to the span wise velocity for the rotor with two towers(Fig. 11), but has a higher order of magnitude. This might be the reason why the wake shape are similar to the wake in Fig. 10, but more spread out. Unfortunately, the vertical velocity component could not be obtained, which could have lead to interesting observations

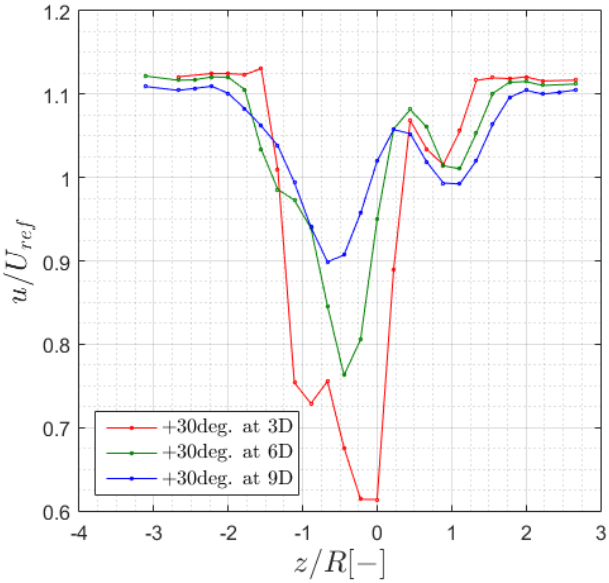

Fig. 16. The wake velocity behind the rotor for $\gamma = +30°$.

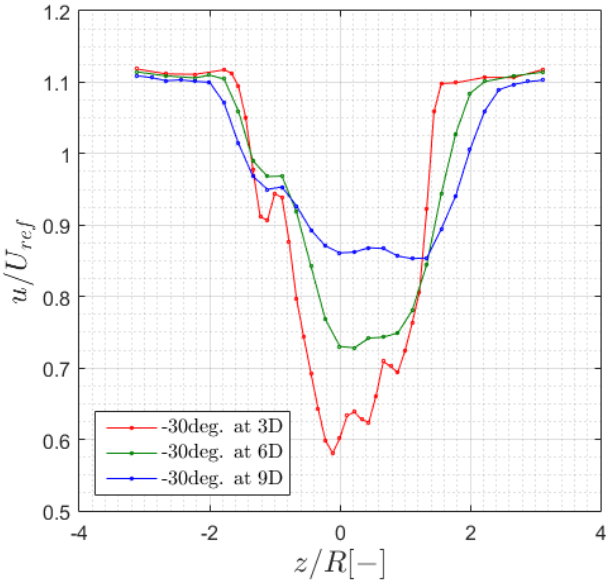

Fig. 17. The wake velocity behind the rotor for $\gamma = -30°$.

and potentially explained the downwards movement of the wake.

For $\gamma = -30°$ in Fig. 13 and Fig. 15, the wake is less complex. The wake centre is slightly below the origin and has the same width as for $\gamma = +30°$. Unlike Fig. 14, the whole wake is within the height of the rotor and is therefore described as flat.

Fig. 15 shows that the span wise velocity is similar to the span wise velocity for the disc in Fig. 9. Hence, it is possible that this setup produces counter-rotating vortices as for the disc. However, the wake does not have the same curled shape as the disc, so differences are expected. To obtain the vertical velocity component is therefore of interest for the future.

The wake behaves slightly different during shear flow conditions at hub height, and it is therefore desirable to measure a 2-dimensional wake profile to see the complete wake at this condition.

To check if the same phenomena is happening at other locations downstream and for other angles of yaw, horizontal wake profiles at $y = 0$ has been measured. Fig. 16 shows the wake profiles for $\gamma = +30°$ at $x = 3D$, $6D$ and $9D$, and Fig. 17 shows the wake profiles for $\gamma = -30°$ at the same locations. These plots show clearly that the wake profiles during $\gamma = +30$ are slimmer than for $\gamma = -30$ at other distances. Also, at $\gamma = +30$ there is a second hump to the right, which is resulting from the hub, just as in Fig. 12. The wakes for positive yaw is also shifting more to the side compared to the opposite direction, as shown earlier.

Horizontal wake profiles at $6D$ for $\gamma = 0°$, $+20°$ and $+40°$ are plotted in Fig. 18, and for $\gamma = 0°$, $-20°$ and $-40°$ in Fig. 19. It is clear that wake profile gets slimmer for higher values of positive yaw, in addition to a more deflected wake centre. This is however not the case for negative yaw-values

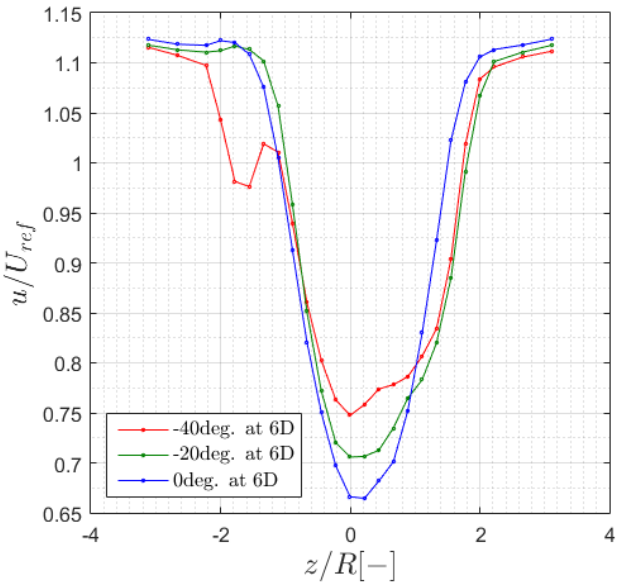

Fig. 18. The wake velocity behind the rotor at 6D for positive yaw (γ).

when the profiles get wider for increased angles of yaw. The complexity of the wake should be kept in mind, and a full 2-dimensional wake measurement is needed to fully understand the influences caused by adjusting the angle. Nevertheless, the plots indicate that the earlier shown differences between directions are kept.

The wake profiles during turbulent and shear flow are shown in Fig. 20 and Fig. 21 for $\gamma = +30°$ and $\gamma = -30°$, respectively. In general, the same differences apply for these condi-

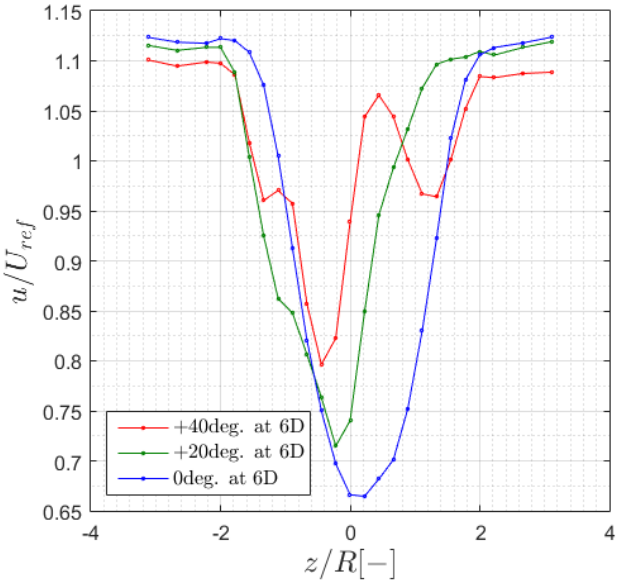

Fig. 19. The wake velocity behind the rotor at 6D for negative yaw (γ).

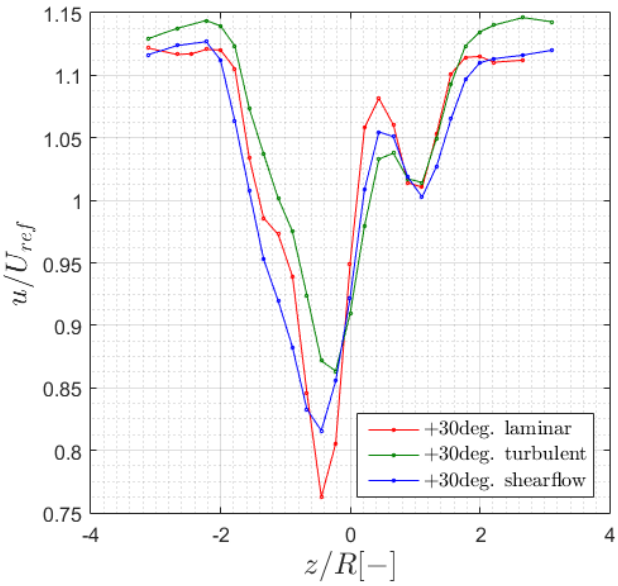

Fig. 20. The wake velocity behind the rotor during different conditions, $\gamma = +30°$.

tions as well. It is shown that the wakes recover faster during turbulent conditions, as expected due to mixing. Regarding the shear flow condition, the wake is the widest for positive angles of yaw, and barely the most narrow for negative angles of yaw. Therefore it is possible that the differences between the yaw directions are smaller for shear flow conditions. Moreover, the shear flow measurements are slightly the most deflected wake in both plots. All the findings during shear flow conditions are

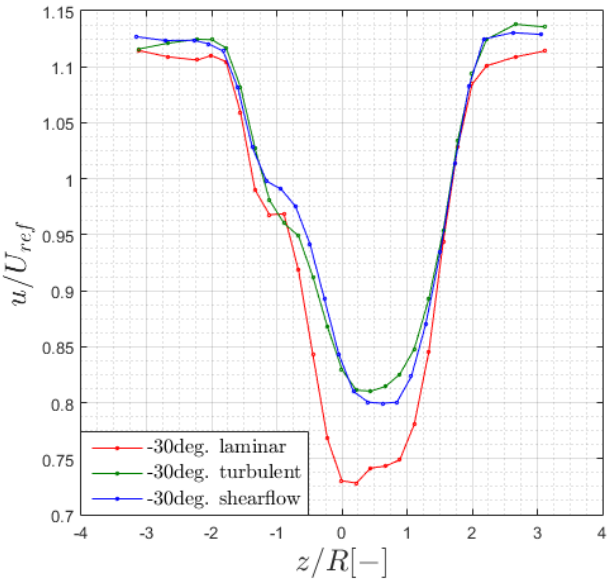

Fig. 21. The wake velocity behind the rotor during different conditions, $\gamma = -30°$.

also represented at 9D(not shown) as a validation, and further investigation is of interest.

IV. Conclusion

In this study, the differences of the wake behind a disc and a rotating rotor in yaw have been investigated. It was found that the wake behind a disc has a symmetric curled shape caused by counter-rotating vortices similar to the the shape of a jet in a crossflow. During the chosen setup, the wake behind a disc deflects significantly more than the wake behind the rotor, and the counter-rotating vortices are in-existent when using the rotor.

Furthermore, the investigation of wake behaviour at the different yaw-directions has taken place. The wake spreads out for positive angles of yaw, and deflects from the centre. Moreover, the wake is wide and flat for negative angles of yaw, and stays closer to the centre. This behaviour is indicated at other downstream distances, as well as for other values of yaw. Moreover, the difference seems to be slightly less affected by the yaw-direction for shear flow conditions, in addition to having a minor increase of sideways deflection.

V. Suggestions to further research

The hub and towers in this study causes strong effects to the wake, hence, it is suggested to investigate the effects by using smaller turbines for the chosen rotor size. This will expectantly give a better understanding of the importance of the physical dimensions regarding the tower and hub.

In order to track and investigate the counter-rotating vortices, it is suggested to measure the velocity component in z-direction. This will hopefully lead to answers regarding

the reason to wake behaviours, especially for yawing in the negative direction where a span wise velocity is present.

To get a better understanding of the wake behaviour during shear flow conditions, it is suggested to measure the wake in a 2-dimensional cross section. This will hopefully yield explaining results relevant for real wind conditions.

ACKNOWLEDGMENT

The author would like to thank supervisor Lars Sætran and co-supervisor Jan Bartl for excelent guidens and fruitful discussions throughout the project. A thank you to Franz Mühle for designing the rotor is also eligible.

REFERENCES

[1] S. Frandsen, R. Barthelmie, S. Pryor, O. Rathmann, S. Larsen, J. Højstrup, and M. Thøgersen, "Analytical modelling of wind speed deficit in large offshore wind farms", Wind Energy, vol. 9, pp. 39–53, 2006.

[2] J. Meyers, C. Meneveau, "Optimal turbine spacing in fully developed wind farm boundary layers," Wind Energy, vol 15, pp. 305-317, 2012.

[3] K. S. Hansen, R. J. Barthelmie, L. E. Jensen, and A. Sommer, "The impact of turbulence intensity and atmospheric stability on power deficits due to wind turbine wakes at horns rev wind farm", Wind Energy, vol. 15, pp. 183–196, 2012.

[4] P. McKay, R. Carriveau, D. S-K. Ting, "Wake impacts on downstream wind turbine performance and yaw alignment", Wind Energy, vol 16, pp. 221-234, 2013.

[5] M. S. Adaramola, P-Å Krogstad, "Wind tunnel simulation of wake effects on wind turbine performance", Proceedings of European Wind Energy Conference, Warsaw, Poland, 2010.

[6] D. Medici, P. H. Alfredsson, "Measurements on a Wind Turbine Wake: 3D Effects and Bluff Body Vortex Shedding", Wind Energy, Vol 9, pp. 219-236, 2006.

[7] M. S. Adaramola, P-Å Krogstad, "Experimental investigation of wake effects on wind turbine performance", Renewable Energy 36, pp. 2078-2086, 2011.

[8] A. Ozbay, W. Tian, Z. Yang, H. Hu, "Interference of Wind Turbines with Different Yaw Angles of the Upstream Wind Turbine", 42nd AIAA Fluid Dynamics Conference and Exhibit, 2012.

[9] P-Å Krogstad, M. S. Adaramola, "Performance and near wake measurements of a model horizontal axis wind turbine", Wind Energy, Vol 15, pp. 743-756, 2012.

[10] M. Bastankhah, F. Porté-Agel, "A wind-tunnel investigation of wind-turbine wakes in yawed conditions", Journal of Physics: Conference Series 625 (2015) 012014, 2015.

[11] T. Mikkelsen, N. Angelou, K. Hansen, M. Sjöholm, M. Harris, C. Slinger, P. Hadley, R. Scullion, G. Ellis, G. Vives, "A spinner-integrated wind lidar for enhanced wind turbine control", Wind Energy, Vol 16, pp. 625-643, 2013.

[12] P. A. Fleming, P. M.O. Gebraad, S. Lee, J-W. van Wingerden, K. Johnson, M. Churchfield, J. Michalakes, P. Spalart, P. Moriarty,"Evaluating techniques for redirecting turbine wakes using SOWFA", Renewable Energy 70, pp. 211-218, 2014

[13] P. M. O. Gebraad, F.W. Teeuwisse, J.W. van Wingerden, P. A. Fleming, S. D. Ruben, J. R. Marden, and L. Y. Pao, "A Data-Driven Model for Wind Plant Power Optimization by Yaw Control", American Control Conference, 2014.

[14] Á. Jiménez, A. Crespo, E. Migoya, "Application of a LES technique to characterize the wake defl ection of a wind turbine in yaw", Wind Energy, Vol 13, pp. 559-572, 2010.

[15] M. F. Howland, J. Bossuyt, L. A. Martínez-Tossas, J. Meyers, C. Meneveau, "Wake Structure of Wind Turbines in Yaw under Uniform Inflow Conditions", PREPRINT, submitted to the Journal of Renewable and Sustainable Energy, 2016.

[16] G. T. Maal, "Parameter study of two in-line model wind turbines in a shear flow", Norwegian University of Science and Technology NTNU, 2014.

[17] T. Bracchi, P-Å. Krogstad, "Yaw Moments of a Three-axis Wind Turbine with Yaw Error", International Offshore and Polar Engineering Conference, Proceedings of the Twenty-second, pp. 248-254, 2012.

[18] F. E. Jørgensen, "How to measure turbulence with hot-wire anemometers", Dantec Dynamics, 2002

[19] F. Pierella, P-Å. Krogstad, L. Sætran, "Blind Test 2 calculations for two in-line model wind turbines where the downstream turbine operates at various rotational speeds", Renewable energy, vol 70, pp. 62-77, 2014.

[20] K. Mahesh, "The Interaction of Jets with Crossflow", Annual Review of Fluid Mechanics, vol 45, pp. 379-407, 2012.

[21] Y. Kamotani, I. Greber, "Experiments on turbulent jet in a crossflow", AIAA, vol 10, pp. 1425–1429, 1972.